J Mol Model (2003) 9:114–123
DOI 10.1007/s00894-003-0123-3

ORIGINAL PAPER

Feng Sun

Molecular dynamics simulation of human immunodeficiency virus protein U (Vpu) in lipid/water Langmuir monolayer

Received: 26 September 2002 / Accepted: 28 January 2003 / Published online: 2 April 2003

Abstract Virus protein U (Vpu) is an accessory membrane protein encoded by human immunodeficiency virus type 1 (HIV-1). Various NMR and CD studies have shown that the transmembrane domain of Vpu has a helical conformation and that the cytoplasmic domain adopts the helix-loop-helix-turn motif. This 3.5-ns molecular dynamics (MD) simulation of Vpu in a lipid/membrane environment has fully reproduced these structural characteristics. Membrane propensities of two amphipathic helices in the cytoplasmic domain are further compared here to understand better their complicated orientational behavior known from experiment. This study first reveals that the highly conserved loop region in the cytoplasmic domain can be closely associated with the membrane surface. It is known from the simulation that Vpu is associated with 34 lipids in this Langmuir monolayer. The lipids that are located between the Vpu transmembrane helix and the first helix in the cytoplasmic domain are pushed up by Vpu. These elevated lipids have increased P–N tilt angles for the head groups but unchanged acyl-chain tilt angles compared with lipids that do not interact with Vpu. This study verifies the significance of applying MD simulation in refining protein structure and revealing detailed protein–lipid interaction in membrane/water environment.

Keywords Vpu · HIV-1 · Langmuir monolayer · Molecular dynamics

Introduction

Virus protein U (Vpu) is a 9.1-kDa integral oligomeric membrane protein encoded by human immunodeficiency virus type 1 (HIV-1). [1, 2] As an accessory protein of HIV-1, Vpu can be deleted without completely abrogating the ability of the virus to replicate in tissue culture. However, the conservation of Vpu in most known HIV-1 isolates indicates its important role in the virus life cycle. [3] Vpu protein has about 80–86 amino acids depending on the viral isolates. [4, 5] The Vpu N-terminal transmembrane (TM) domain serves as a hydrophobic membrane anchor and its polar C-terminal domain is located in the cytoplasm. [6]

The Vpu TM (VpuTM) domain has about 27 amino acids that form a regular linear α-helix in a lipid bilayer with a tilt angle of $\leq 30°$ with respect to the membrane normal. [7, 8] The Vpu cytoplasmic (VpuCyto) domain has about 54 residues containing two helical regions connected by a loop, which contains a highly conserved region Vpu^{52-57}. [4] Several functions of Vpu have been identified and correlated to the structural domains of this protein. The VpuTM domain is associated with the functions of Vpu in enhancing virion release from the infected cells and forming cation-selective channel. This function of Vpu is nonspecific because noninfectious particles or other virus, such as HIV-2, Moloney murine leukemia virus, and SIV can be released as efficiently as HIV-1 particles. [9, 10] Vpu has another function in the degradation of CD4 protein in the endoplasmic reticulum and this function is initiated by physical binding between the VpuCyto domain and CD4. The phosphorylation of two serine groups in the loop region, Ser52 and Ser56, is necessary for CD4 degradation after the initial binding. Vpu-induced CD4 degradation is highly specific and the VpuCyto domain targets sequences located between amino acids 402 and 420 in CD4 cytoplasmic domain. [11, 12, 13]

The functions of VpuTM anchor and VpuCyto domain have also been investigated by various mutation studies. A mutant containing a scrambled VpuTM domain with a conserved amino acid composition and α-helical structure is unable to enhance the release of virus particles from infected or transfected cells or form ion channels. [10, 14] The deletion of two to five amino acids from the N-

F. Sun (✉)
Department of Chemistry,
University of Pennsylvania,
Philadelphia, PA, 19104, USA
e-mail: fengsun1@hotmail.com
Tel.: +1 410-9971229
Fax: +1 410-9971229

terminal, middle or C-terminal parts of the VpuTM domain also impairs Vpu's ability to enhance viral particle release. These results demonstrate that the structural integrity of the VpuTM domain is critical for Vpu's functions in facilitating virion release and the formation of ion channels. [9, 15] For Vpu-induced CD4 degradation, it has been shown that truncation of the last six C-terminal amino acids of the VpuCyto domain results in the inability of Vpu to bind and degrade CD4. [16] The S52N-S56N mutant, with double mutations on two phosphorylation sites, has also lost the ability to induce CD4 degradation. Therefore, the CD4-degradation function of Vpu also depends on the sequences present in the cytoplasmic domain of Vpu and in particular, requires the phosphorylation of two highly conserved serine residues at positions 52 and 56. [11, 14, 17]

A number of high-resolution NMR, solid-state NMR and CD spectroscopic studies have been carried out to obtain the secondary-structure composition and tertiary folding of full-length Vpu and its different regions. Various experimental conditions were used in these experiments, such as lipid bilayers, trifluoroethanol (TFE)/water mixtures, which usually can stabilize the secondary structure of the protein, and high salt solutions. It has been known from these experiments that in lipid bilayers, VpuTM$^{6-27}$ forms a helix that lies almost parallel to the bilayer normal. In aqueous TFE solutions, however, synthetic peptide Vpu$^{1-39}$ adopts a U-shaped structure with residues Ile16–Ala18 in the interconnection region. [7, 8] CD data and NOE signals measured from NMR have been obtained for nine overlapping 15-amino-acid fragments and three longer fragments of the VpuCyto domain in 50% TFE solutions. The experimental data indicate that the VpuCyto domain contains two helices roughly bounded by residues 30–50 and 57–69, respectively, and a single reverse turn at residues 74 to 77. [18] The peptide Vpu$^{32-81}$, which corresponds to the cytoplasmic domain of Vpu, adopts a helix-loop-helix-turn motif in TFE solution, as found from a 2D ^{1}HNMR study. Two helices in this motif, CytoHelix1 and CytoHelix2, are positioned approximately between residues 34–50 and 61–70, and the turn is centered at residue Pro75. [19] In 620-mM salt solution, the peptide Vpu$^{39-81}$ has a well-defined amphipathic α-helix at residues 39–49, a less well-defined helix at 59–67 and a short α-helix at the C-terminal 74–78 known from NMR investigations. [20]

For the orientation of the two helices in the VpuCyto domain, consistent results from solid-state NMR studies have been obtained on CytoHelix1's parallel orientation toward the membrane surface in full length Vpu or in peptide Vpu$^{27-57}$. [6, 7] On the other hand, CytoHelix2 displays different orientational properties in these experiments. In full-length Vpu, CytoHelix2 is parallel to the membrane surface, whereas in the Vpu$^{51-81}$ peptide, this helix has nonpreferred polypeptide orientation and lacks strong interaction with the membrane. Therefore, the exact structure, location and topology of the Vpu cytoplasmic domain in a membrane environment still remain to be explored further, both experimentally and theoretically.

As an integral membrane protein that forms oligomers, Vpu resembles a number of virus-encoded proteins, such as influenza M2, Semliki Forest virus 6K and poliovirus 2B and 3A proteins. [21, 22, 23] Expression of these proteins in bacterial cells enhances the membrane permeability because of their channel activity. The elucidation of structural characteristics of Vpu in a membrane environment may help to understand the mechanisms of the functions of Vpu and its structurally related viral proteins. Knowledge of the secondary structure compositions and the alignment of α-helical regions with respect to the membrane surface provides a guideline for constructing functional oligomers of these membrane proteins in future studies.

Currently available experimental results on the Vpu structure give a good starting point for further molecular dynamics (MD) investigations. The effectiveness of the MD simulation can be verified by reproducing the protein structure obtained from various experiments. Then, complementary knowledge on protein structure and protein–lipid interaction in the membrane/water environment may be derived from the simulation. In this study, a constant normal pressure, constant surface tension and constant temperature ($NP_N\gamma T$) molecular dynamics simulation has been performed on full-length Vpu in a lipid/water Langmuir monolayer at room temperature and 22.9-mN/M surface tension. 1,2-Dilignoceroylphosphatidylcholine (DLGPC) was chosen in this study to form a lipid Langmuir monolayer on the water surface. A DLGPC molecule has two saturated 24-carbon acyl chains and the hydrocarbon core thickness of this monolayer is about 2.8 nm. This thickness is close to the hydrocarbon core thickness of a membrane of a living system. $NP_N\gamma T$ MD simulation on DLGPC/water monolayer system showed that this monolayer in the liquid-condensed phase shares many structural characteristics with typical short-chain 1,2-diacylphosphtidylcholine systems, such as a DPPC/water monolayer in the condensed phase and a DPPC/water bilayer in the gel phase. [24] In this paper, secondary structure compositions and orientations of three helices in Vpu obtained from Vpu/DLGPC/water MD simulations were first compared with available experimental data to verify the validity of this $NP_N\gamma T$ MD simulation. Then, MD results from Vpu$^{27-57}$/DLGPC/water and Vpu$^{51-81}$/DLGPC/water systems were used to understand better different experimental results on the orientation of CytoHelix2. Next, the amphipathicity of two VpuCyto helices was investigated to yield more knowledge on the hydrophobic/hydrophilic characteristics of these helices instead of only helical-wheel diagrams being applied, as in many experimental studies. Then, new findings revealed by the MD simulations on the Vpu structure in the membrane/water environment are presented, such as the close association between the cytoplasmic loop and membrane surface, and good conformational stability of Vpu. Finally, atomic level

protein–lipid interactions in Vpu/DLGPC/water system are revealed for the first time by the MD study.

Materials and methods

System setup

A DLGPC/water monolayer was constructed according to Sun. [24] 144 DLGPC molecules were used to form a monolayer comprising a surface with area about 11 nm×6 nm=66nm^2. After this DLGPC/water monolayer underwent 500 ps of $NP_N\gamma T$ MD simulation, six DLGPC molecules were removed from the monolayer to form a hole to accommodate the Vpu protein. The sequence of full-length Vpu used in the simulation is: QPIQIAIVAL VVAIIIAIVV WSIVIIEYRK ILRQRKIDRL IDRLIERAED SGNESEGEIS ALVELGVELG HHAPWDVDDL. Based on NMR and CD information about this protein, which is most helical, the initial structures of the VpuTM and VpuCyto domains were obtained using InsightII (Accelrys Inc., San Diego, Calif.) with residues set in α-helical conformations. Constant volume, constant temperature (*NVT*) simulation was used for each domain in vacuum for 20 ps. According to the known vertical orientation of the VpuTM domain and parallel orientation of the VpuCyto domain with respect to the membrane surface, the VpuTM and VpuCyto domains obtained after *NVT* simulation were then combined to form an L-shaped full-length Vpu with the N- and C-termini being acetylated and amidated, respectively. Next, the upper half of VpuTM domain was inserted into the hole in the monolayer (Fig. 1a). After 15 ps *NVT* simulation on the Vpu/DLGPC system, the entire VpuTM domain had entered into the DLGPC monolayer. A box of 7,330 TIP3 waters was subsequently added to the Vpu/DLGPC monolayer to solvate the system. Those water molecules within a 0.35-nm sphere of an atom in the peptide or lipids were deleted. Six Na^+ counterions were added to the Vpu/DLGPC/water system by replacing water molecules to ensure the overall neutrality of the simulated system. The total number of atoms in the system was 47,868.

For the Vpu$^{27-57}$/DLGPC/water and Vpu$^{51-81}$/DLGPC/water systems, VpuCyto in vacuum was truncated to yield the peptides Vpu$^{27-57}$ and Vpu$^{51-81}$. In these two peptide systems, each peptide has a similar initial orientation toward the membrane surface as its corresponding region in full-length Vpu. The structures of all the systems were visualized using the program RASMOL [25].

Equilibration

After vacuum *NVT* simulation of the full-length Vpu, loop, CytoHelix2 and tail regions are less structured than VpuTM and CytoHelix1 (Fig. 1a). During the subsequent $NP_N\gamma T$ simulation on the Vpu/DLGPC/water system, VpuTM and CytoHelix1 maintain good helicity. CytoHelix2 also adopts a helical conformation in the lipid/water environment (Fig. 1b, c). Loop and tail regions are not able to form the helical conformation throughout the simulation. After 2 ns simulation, the system has constant helical composition and the three helices in Vpu show no drift in orientation angle (Fig. 2). The total $NP_N\gamma T$ simulation length is 3.5 ns. The lipid acyl-chain and head-group reach equilibrium tilt angles, 29.4±3.7° and 76.3±24.3°, respectively, after 2.9 ns simulation. Therefore, the system was considered to be in equilibrium after 2.9 ns. The analysis data were collected during the last 350 ps simulation in 0.5-ps intervals to yield 700 structures. 3 ns of $NP_N\gamma T$ MD simulation was performed for each of the Vpu$^{27-57}$/DLGPC/water and Vpu$^{51-81}$/DLGPC/water systems to yield equilibrium configurations.

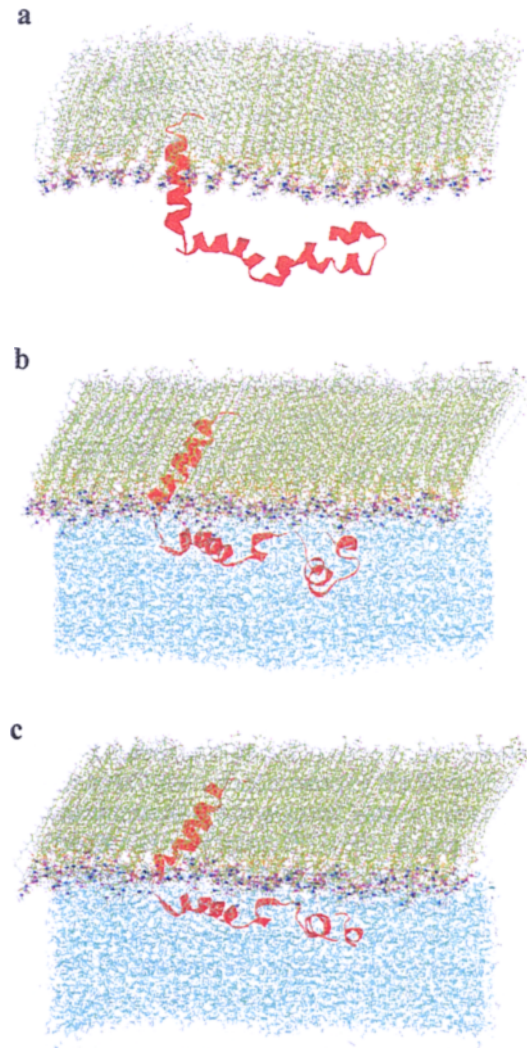

Fig. 1 **a** *XZ* view of the initial configuration of Vpu with the upper half of VpuTM domain inserted into the monolayer. **b** *XZ* view of a snapshot of Vpu/DLGPC/water system after 1 ns $NP_N\gamma T$ MD simulation. **c** *XZ* view of a snapshot of Vpu/DLGPC/water system after 3.5 ns $NP_N\gamma T$ MD simulation. Coloring scheme: Vpu, *red*; C, *green*; H, *pink*; N, *blue*; O, *orange*; P, *magenta*; water, *light blue*

Molecular dynamics simulations

The simulations were carried out using CHARMM27 and the CHARMM27 all-atom topologies and force fields. [26, 27] For *NVT* MD simulations, the Nosé–Hoover method was used to control the temperature of the system with the thermal inertial parameter set to 50. [28, 29] The algorithms for performing constant normal pressure and surface tension simulation as used in the $NP_N\gamma T$ ensemble have been described by Zhang et al. [30] Three-dimensional periodic boundary conditions were used and the length of the simulation cell normal to the monolayer was set to be large enough, 25 nm, to ensure that the interactions between periodic replicas in this direction are negligible. Particle-mesh Ewald was applied to calculate the electrostatic energies and forces with approximately 0.1-nm grid spacing for the fast Fourier transform. The van der Waals interactions were calculated with simple truncation at 1.2 nm. The distance between any two atoms, one in Vpu and the other in the Vpu images, is larger than twice the van der Waals cutoff. Therefore, there is no protein–protein

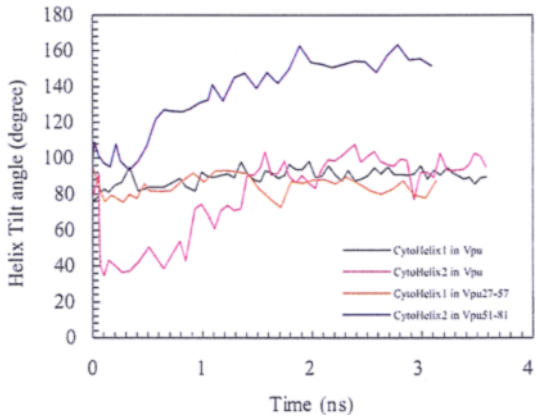

Fig. 2 Helix tilt angles of two VpuCyto helices versus simulation time with respect to the monolayer normal in full-length Vpu, Vpu^{27-57} and Vpu^{51-81} systems

interaction in this combined protein/membrane system. The SHAKE algorithm was used to constrain the lengths of bonds involving hydrogen atoms. The time step used in the simulation was 2 fs. 1 atm normal pressure, 22.9 mN/M surface tension and 293.15 K were used as the simulation conditions.

Results

Residues included in various helices of Vpu

In Fig. 1, the configurations of Vpu in a DLGPC/water Langmuir monolayer are shown at different simulation stages. The simulation yields three helical regions in full length Vpu. These helical regions can be verified from Φ/Ψ plots of the residues in each helix (Fig. 3). It was found that the helix in the VpuTM domain includes residues Gln5 to Ile26 and CytoHelix1 contains residues Ile32 to Glu47, according to their Φ and Ψ angles. Although residues Glu59 and Glu69, which are located at the termini of CytoHelix2, have Φ/Ψ angles that deviate from a helical Φ/Ψ region, hydrogen bonds were found between the carbonyl of Glu59 or Val64 and the amide of Leu63 or Glu69, respectively. The donor–acceptor distance and H-donor–acceptor angle in Glu59–Leu63 are 0.337±0.041 nm and 24°, respectively. Val64–Glu69 has a donor–acceptor distance of 0.283±0.014 nm and a H-donor-acceptor angle of about 13°. These distances and angles satisfy the criteria for assigning a hydrogen bond according to Forrest et al. [31] Therefore, residues Glu59 and Glu69 are also included in CytoHelix2. Table 1 gives the residue compositions of each helix in Vpu from both the MD simulation and various experiments.

As can be noted from Table 1, the residues included in each helix of Vpu were reproduced well in the MD simulation except for the terminal residues of the helices, which may have various conformations, depending on the conditions. NMR data suggest that in a membrane environment, the N-terminus of the VpuTM helix does not begin before residue Gln5 or Ile6 but is present by or before residue Ala10, and the C-terminus of this helix ends between Trp22 and Tyr29. [8] It is verified in this MD simulation that this helix starts from Gln5 and is 22 residues long in the lipid membrane. Similar to the lipid bilayer, the U-shaped structure of the VpuTM domain measured in TFE solution was also not observed in this Vpu/DLGPC/water system. In experimental studies, the structure of the VpuCyto domain was mainly obtained from solution NMR and CD spectroscopy by measuring various peptides corresponding to various regions of Vpu. [18, 19, 20, 32] The experimental results indicate the existence of two helical regions in the VpuCyto domain, although each helix may have varied terminal residues as various solutions or peptides were used. This Vpu/DLGPC/water MD simulation results in a helix-loop-helix motif adopted by residues 32–69 in the VpuCyto domain and this conformation is consistent with the experimental findings.

Orientations of various helices with respect to the membrane surface

The orientation of a helix in a membrane environment is described by the helix tilt angle, which is the angle the average the N–H vector of residues in the helix makes with the membrane normal. For the VpuTM helix, residues 5–20, which are embedded in the hydrophobic

Table 1 Residues included in each helix of Vpu from Vpu/DLGPC/water MD simulation and various experiments

	MD	Experimental
VpuTM helix	Gln5–Ile26	~Ile6–Ile27 (estimated) in lipid bilayer[a] A U-shaped structure in TFE/water solution, unable to span a bilayer[a]
CytoHelix1	Ile32–Glu47	~Arg30–Ala49 in lipid bilayer[b] ~Arg34–Glu50 in TFE/water solution[c] ~Asp39–Ala49 in high salts solution[d]
CytoHelix2	Glu59–Glu69	~Gly58–Leu70 in lipid bilayer[b] ~Glu57–Glu69 in TFE/water solution[c] ~Glu59–Gly67 in high salts solution[d]

[a] From Wray et al. [8]
[b] From Ma et al. [32]
[c] From Wray et al.; [18] Federau et al. [19]
[d] From Willbold et al. [20]

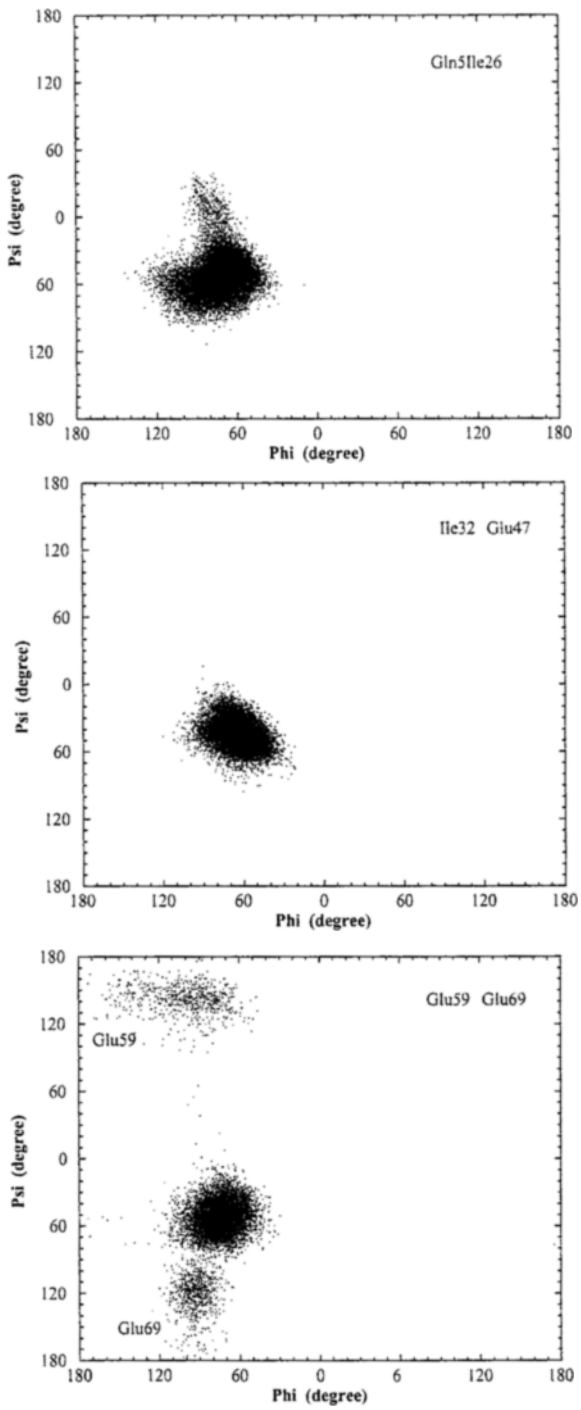

Fig. 3a–c Φ/Ψ plots of the 700 structures obtained in 0.5 ps intervals from the last 350 ps simulation on Vpu/DLGPC/water system. **a** Gln5–Ile26, **b** Ile32–Glu47, and **c** Glu59–Glu69

core of the monolayer, were used to calculate the helix tilt angle. All residues in CytoHelix1 and CytoHelix2 were included in the calculation of the tilt angle of each helix. Table 2 gives the tilt angles of the three helices in Vpu from the MD simulation and experiments. This table shows that the overall topology of full-length Vpu in a DLGPC/water Langmuir monolayer from the MD study agrees very well with that in lipid bilayers measured by the solid NMR experiments. The difference in the tilt angle of the VpuTM helix in monolayer and bilayer may come from only one head group region existing in a monolayer instead of two in a bilayer.

As listed in Table 2, CytoHelix2 was measured to have a nonpreferred orientation in the peptide Vpu^{51-81} system, although it is parallel to the membrane surface in full-length Vpu. In contrast, CytoHelix1 is parallel to the membrane in both the Vpu and Vpu^{27-57} systems. MD simulation on two additional peptide systems, Vpu^{27-57}/DLGPC/water and Vpu^{51-81}/DLGPC/water, may shed light on the orientation of the cytoplasmic helices of Vpu. Figure 4 shows the instantaneous configurations of two systems after 3 ns $NP_N\gamma T$ MD simulation. As revealed by the simulation, CytoHelix1 remains in a parallel orientation in the peptide Vpu^{27-57} system but the orientation of CytoHelix2 in the peptide Vpu^{51-81} is quite different from that in full-length Vpu. The tilt angles of CytoHelix1 and CytoHelix2 in full-length Vpu, Vpu^{27-57} or Vpu^{51-81}, as a function of simulation time are shown in Fig. 2. From this figure, it can be observed that the tilt angle of CytoHelix2 in Vpu^{51-81} changes from an initial ~90° to a final ~150° during 3 ns of MD simulation. CytoHelix2 in the peptide Vpu^{51-81} system is much less associated with the membrane surface than that in the full-length Vpu system (Fig. 1c; Fig. 4b). The center-of-mass distances between various regions of the VpuCyto domain in the Vpu/DLGPC/water system, and the membrane surface are shown in Table 3. The position of the membrane surface is defined by the average positions of P and N atoms in the lipid head groups.

From Table 3, it is known that CytoHelix1 has good affinity for the membrane surface because there is only ~0.8 nm distance between the center of mass of this helix and lipid head groups. Therefore, CytoHelix1 maintains a parallel orientation in both the full-length Vpu and the Vpu^{27-57} peptide systems, as MD simulation and experiments reveal. As can be found in Table 3, the Vpu^{52-57} loop also interacts strongly with the membrane surface in the full-length Vpu. However, CytoHelix2 does not have a strong affinity for the membrane surface and is ~0.5 nm away from the membrane, compared with CytoHelix1 in

Table 2 Tilt angles of Vpu helices from Vpu/DLGPC/water MD simulation and different bilayer experiments

	MD	Experimental
VpuTM helix	36.5±2.4°	≤30° [a,b]
CytoHelix1	90.6±2.5°	~90° in full-length Vpu or Vpu^{27-57} [a,b]
CytoHelix2	96.4±5.5°	~90° in full-length Vpu[a] Nonpreferred orientation in Vpu^{51-81} [b]

[a] From Marassi et al. [7]
[b] From Henklein et al. [6]

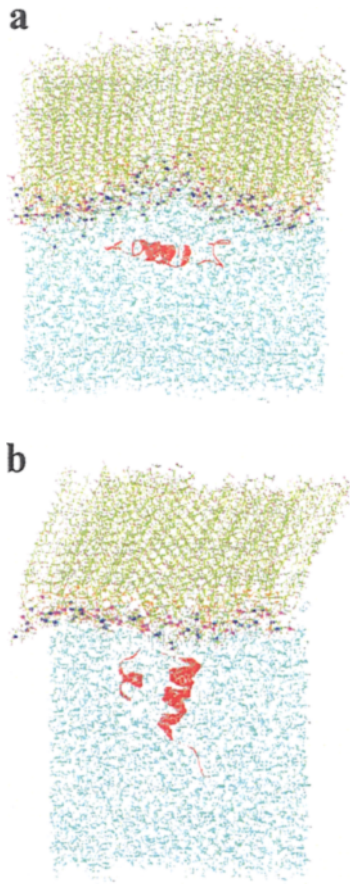

Fig. 4 **a** *XZ* view of a snapshot of Vpu^{27-57}/DLGPC/water system after 3 ns simulation with N-terminus on the left. **b** *XZ* view of a snapshot of Vpu^{51-81}/DLGPC/water system after 3 ns simulation with Vpu tail on the left. For the coloring scheme, see caption of Fig. 1

Table 3 Center-of-mass distances between various regions of VpuCyto domain and the membrane surface in full-length Vpu/DLGPC/water system

	Center-of-mass distance (nm)
CytoHelix1	0.796
Vpu^{52-57} loop	0.580
CytoHelix2	1.310
Tail	1.220

full-length Vpu. Both experiment and simulation demonstrate that CytoHelix2 is parallel to the surface in full-length Vpu while it has a nonpreferred orientation in the peptide Vpu^{51-81}. These results indicate that the orientation of this helix is affected by other regions in the polypeptide. In the full-length Vpu system, because both CytoHelix1 and the loop region have strong interaction with the membrane surface, they may generate a constraint on the orientation of CytoHelix2. With the presence of CytoHelix1 and the loop region in full-length Vpu, a parallel orientation of CytoHelix2 is favored. In the Vpu^{51-81} peptide system, however, the loop region is far away from the membrane surface, as can be found in

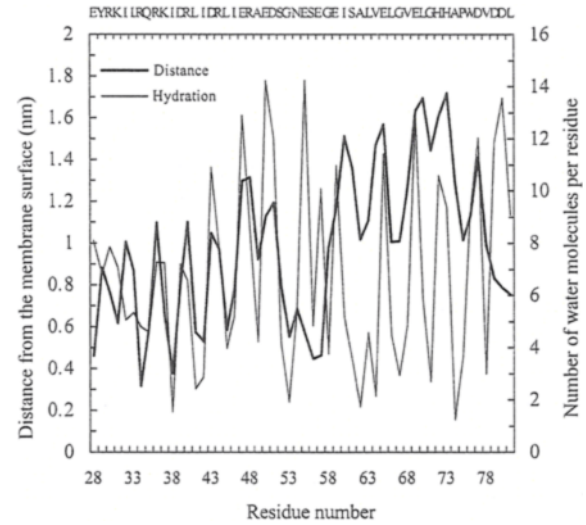

Fig. 5 The center-of-mass distance between the residue and the membrane surface, and the number of water molecules within 0.25 nm of any atom of the residue as the functions of the residue number in VpuCyto domain of full-length Vpu system. These values were obtained from 700 structures collected in the last 350 ps simulation

Fig. 4b. Without the constraint from its preceding regions, CytoHelix2, which lacks the high affinity for the membrane, can have various orientations toward the membrane surface in the Vpu^{51-81} peptide system. The MD study indicates that different experimental results on the orientation of CytoHelix2 are because of this helix's weak affinity for the membrane surface and different peptides being used in different experiments. It was also observed from MD that the Vpu tail region is actually more closely associated with the membrane than CytoHelix2 in the full-length Vpu or Vpu^{51-81} peptide systems (Fig. 1c and Fig. 4b). This finding might provide a reason why CytoHelix2 in the Vpu^{27-57} peptide lacks the fast reorientation, as indicated by solid NMR bilayer study. [6]

Amphipathicity of CytoHelix1 and CytoHelix2

An amphipathic helix has opposing polar and nonpolar faces oriented along the long axis of the helix. For membrane-associated proteins, the amphipathic secondary structure characteristic plays an important role in the biological activity of the polypeptide. Lipid-membrane surfaces provide an amphipathic environment, hydrophilic toward aqueous phase and hydrophobic toward the lipid hydrocarbon chains. An amphipathic helix may bind to the lipid membrane with a high affinity with hydrophobic face associating with the lipids and hydrophilic face interacting with the water molecules. [33, 34, 35] In order to characterize the amphipathicity of two cytoplasmic helices in Vpu, the center-of-mass distances to the membrane surface and the hydration state of all residues in VpuCyto domain were calculated and are

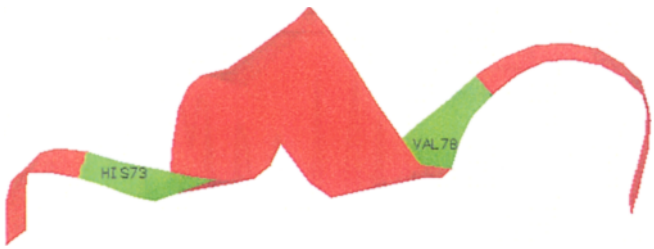

Fig. 6 The turn formed at the Vpu tail region. This turn includes residues from His73 to Val78

shown in Fig. 5. The hydration state of a residue is described by the number of water molecules within a 0.25 nm sphere of any atom in that residue. CytoHelix1 is highly amphipathic from residues Arg36 to Glu47 with hydrophobic side containing residues Ile38, Leu41, Ile42, Leu45 and Ile46. This hydrophobic side is closer to the membrane surface than the hydrophilic side, with average center-of-mass residue distances to the membrane for each side of 0.569 nm and 0.996 nm, respectively. In CytoHelix1, the hydration state of the hydrophobic side is less than that of the hydrophilic side, each having 1.5–5.1 and 6.5–12.8 water molecules/residue, respectively. Therefore, the simulation results illustrate that the amphiphathic CytoHelix1 contacts the membrane surface using its hydrophobic side and its hydrophilic side is solvated by aqueous solution. Residues from Ser61 to Glu69 in CytoHelix2 also fold into an amphipathic helix with a well-hydrated hydrophilic side comprising residues Ser61, Glu65 and Glu69. The amphipathic property of these two helices has been suggested in the experimental studies with the aid of the helical-wheel representation. ^{15}N-labelled solid-state NMR indicates that the hydrophobic side of CytoHelix1 faces the membrane surface. [6] The MD simulation supplies much more detailed information on the distributions of hydrophobic/hydrophilic sides, membrane propensities and hydration states of these two amphipathic helices in the membrane/water environment.

Turn at the Vpu tail

Figure 6 shows the turn formed between His73 and Val78 after Vpu/DLGPC/water MD simulation. The turn determined from MD is consistent with that observed from NMR medium-range NOEs. This study reveals that in this tail-turn region, three hydrogen bonds form between residue pairs, His73–Asp77, His73–Trp76 and Ala74–Val78. The donor–acceptor distances for the above hydrogen bonds are 0.307±0.029 nm, 0.305±0.019 nm and 0.305±0.025 nm, respectively. Combined with the helix-loop-helix structure found earlier for the residues 32–69, the simulation on the full-length Vpu system yields the helix-loop-helix-turn conformation for the VpuCyto domain. The effectiveness of the $NP_N\gamma T$ MD approach in studying the Vpu structure in a membrane/water environment has been confirmed by reproducing Vpu's structure and topology in a membrane environment. The good biological relevance of using DLGPC/water monolayer in the Vpu structural study has also been shown here.

Ser52-Glu57 loop's close association with the membrane surface

From the center-of-mass distances between different regions of Vpu and the membrane surface shown in Table 3, it is known that in the full-length Vpu system, the Vpu^{52-57} loop is the closest to the membrane surface in the VpuCyto domain. This is because a hydrogen bond with a length of 0.268±0.011 nm forms between the hydroxyl group of Ser56 and the phosphate group in DLGPC. Also, the carboxylate group in Glu57 is closely associated with ammonium in the DLGPC head group with a distance between the oxygen atoms in the COO^- group and the hydrogen atoms in the $N(CH_3)_3^+$ group within 0.25–0.35 nm. However, this loop region is not well structured. Therefore, its conformation may vary in various Vpu molecules. This simulation suggests that the loop region is in close proximity of the membrane surface. It is known from experiments that Ser52 and Ser56 need to be phosphorylated for the degradation of the viral receptor CD4. Solid NMR experiments on Vpu^{27-57} point out that phosphorylation on Ser52 and Ser56 weakens the interactions between the CytoHelix1 and the membrane. [6] The simulation agrees with the experimental observation that phosphorylation may weaken the association between the loop and the membrane surface because the hydrogen bond between Ser56 in the loop and lipid cannot form after phosphorylation of the serine groups.

Good conformational stability of Vpu

Root-mean-square deviation (RMSD) values between the 700 structures collected in the last 350 ps of MD simulation at 0.5-ps intervals for the protein backbone and all atoms were calculated to investigate the conformational stability of Vpu. The RMSD was calculated according to:

$$(\mathrm{RMSD})_i = \left\{ \frac{1}{N_a N_f} \sum_{a}^{N_a} \sum_{f}^{N_f} \left(\mathbf{R}_{af} - \langle \mathbf{R}_{af} \rangle \right)^2 \right\}^{1/2} \qquad (1)$$

where $\mathbf{R}_{af}$ is the instantaneous position of atom a in residue i, and $\langle \mathbf{R}_{af} \rangle$ is the average position for this atom. N_a and N_f are the numbers of atoms in the residue i and coordinate frames used in the averages, respectively. From Fig. 7, it can be found that the VpuTM helix, which includes residues Gln5–Ile26, is very stable with all-atom RMSD values less than 0.15 nm. The backbone of

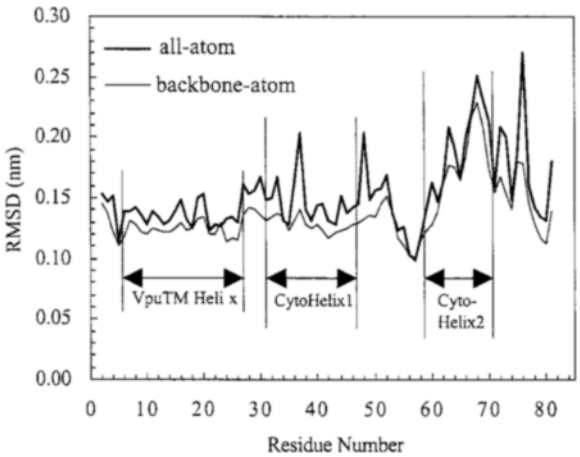

Fig. 7 RMSD values as a function of the residue number for the Vpu/DLGPC/water system. These values were obtained for all and backbone atoms of 700 structures collected in the last 350 ps simulation. Three helical regions are marked by the *arrows*

CytoHelix1 is also very stable, although the side chain of Lys37 fluctuates more. The highly conserved Ser52–Glu57 loop has the lowest RMSD values in the VpuCyto domain, about 0.1 nm RMSD for both backbone and all atoms. The rigid loop region may result from the formation of hydrogen bonds between Ser56 and the lipid, and the close association between Glu57 and the ammonium in the lipid head group. CytoHelix2 shows less stability, especially at its C-terminus, compared with other helices in the Vpu. The tail region has RMSD values usually below 0.2 nm for backbone atoms, but Trp76 has the largest all-atom RMSD value, ~0.27 nm, among all residues in Vpu. This indicates more conformational flexibility in the tail region. The overall RMSD values for backbone and all atoms are less than 0.23 nm and 0.27 nm respectively, indicating good conformational stability of the full-length Vpu in the DLGPC/water Langmuir monolayer.

Influence of Vpu on the structure of DLGPC/water monolayer

The experiments reveal that various regions of Vpu are in the proximity of the membrane. [6, 7, 8] This MD study shows that full-length Vpu is associated with 34 DLGPC lipids, including 12 lipids surrounding the VpuTM domain and 29 lipids right above the VpuCyto domain. There are seven lipids contacting both the VpuTM domain and CytoHelix1. In order to reveal the detailed interactions between various regions of Vpu and the lipid molecules, the lipid molecules associated with each region of Vpu were identified and assembled into one group. Table 4 gives the definition of six selected lipid groups, the number of lipids in each group, average acyl-chain tilt angle, P–N tilt angle, and number of *gauche* states/chain of each group. The P–N tilt angle is defined to be the angle the P–N vector in the lipid head group makes with the surface normal. The acyl-chain tilt angle and *gauche* states/chain were calculated in the same way as used by Sun. [24] These values obtained from the pure DLGPC/water system are also included in the Table 4 for comparison.

Each heavy atom in DLGPC is assigned a number as shown in Fig. 8. In each lipid group, the average position along the membrane normal of each heavy atom was obtained by taking the average of the same heavy atoms in the group over the last 350 ps simulation. Then, the average position differences between Group i, i=1 to 5, and Group 6 for all heavy atoms were obtained and plotted in Fig. 9. Group 6 contains the lipids that are not associated with Vpu. Table 4 indicates that acyl-chain tilt angles in different lipid groups do not vary much from one another although various lipid groups interact with various regions of Vpu. Figure 9 shows that Group 1 lipids, which are located between the VpuTM helix and CytoHelix1, have the largest atomic position difference. The ammoniums in this group are pushed up 0.25–0.3 nm by Vpu compared to those in Group 6. The pushing effect on the lipids in Group 1 gradually decreases for the atoms as they are further away from the membrane/water interface and the limiting elevation value for the methylene carbons is about 0.15 nm. Lipids in Group 2, which surround the other side of the VpuTM helix but without contacting CytoHelix1, do not experience such a pushing

Table 4 Definition, number of lipids, acyl-chain tilt angle, P–N tilt angle and number of *gauche* states per chain in each lipid group in Vpu/DLGPC/water system

Lipid group	Definition	Number of lipids	Acyl-chain tilt angle	P–N tilt angle	*Gauche* states/chain
1	Contacting both VpuTM and CytoHelix1	7	30.2±3.7°	83.3±22.5°	1.1
2	Contacting only VpuTM	5	30.4±2.4°	62.3±31.1°	1.0
3	Above CytoHelix2	7	29.0±1.8°	76.2±19.6°	0.7
4	Above loop	7	28.8±2.2°	79.3±16.1°	0.9
5	Above tail	9	27.8±2.8°	79.9±18.8°	0.6
6	Not associated with Vpu	104	29.6±4.1°	75.9±25.2°	0.6
DLGPC	Pure DLGPC/water system[a]		29.4°	74.6±25.8°	0.5

[a] From Sun [24]

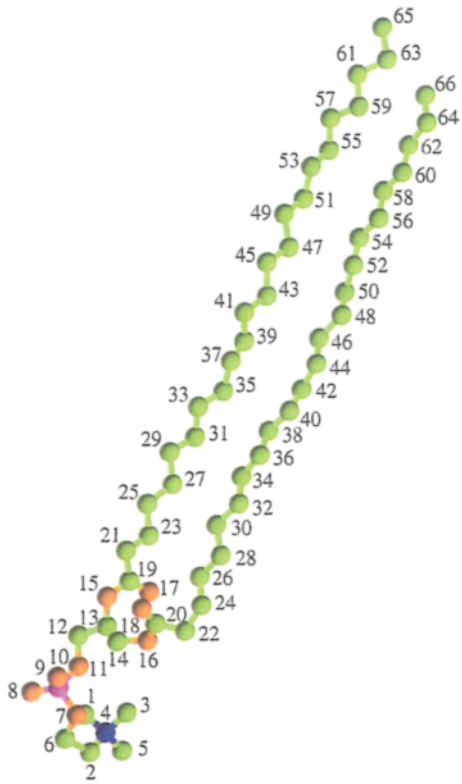

Fig. 8 The atom-numbering scheme used in the text for DLGPC molecule. Numbers 4 and 9 are nitrogen and phosphorus atoms, respectively. Oxygen atoms are: 7, 8, 10, 11, 15, 16, 17 and 18. The other atoms are carbons. For the coloring scheme, see caption of Fig. 1

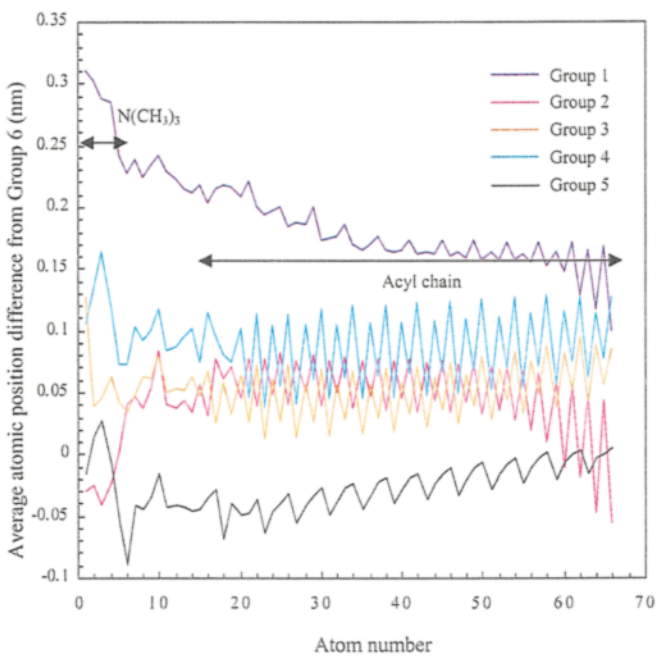

Fig. 9 The average atomic position differences along the monolayer normal between Group i, i=1 to 5 and Group 6, for the heavy atoms of the lipids in the Vpu/DLGPC/water system. The ammonium group and acyl-chain regions are marked by the *arrows*. These values were obtained from 700 structures collected in the last 350 ps of simulation

effect from the Vpu. The lipids in Group 3, 4 or 5 are only associated with the VpuCyto domain and the atomic position differences between these lipids and lipids in Group 6 are usually less than 0.1 nm. From P–N tilt angles for different lipid groups, it is found that the pushing effect on Group 1 lipids is accompanied by an increase in the P–N tilt angle for this group and the decrease in P–N tilt angle for Group 2. There are about 21° differences in the P–N tilt angle between these two groups. It is also observed that the VpuTM domain introduces disorder in its surrounding lipid acyl chains because *gauche* states/chain increases ~0.5 for lipids in Group1 and Group 2 compared with the lipids in Group 6. Group 4 lipids, which contact the loop region, also have increased disorder in the acyl chain, probably because of the hydrogen-bond formation between the loop and the lipids. CytoHelix2 and the Vpu tail region, which are relatively farther away from the membrane surface, have less effect on the lipid conformation. Comparing lipids in Group 6 and lipids in pure DLGPC/water monolayer, it is found that they have similar values of lipid tilt angle, P–N tilt angle and *gauche* states/chain. These similarities imply that the Vpu–lipid interaction is mainly confined between the Vpu protein and its nearest-neighbor lipids under the conditions studied. The overall integrity of the monolayer is maintained after the insertion of the Vpu into this Langmuir monolayer.

Discussion

$NP_N\gamma T$ MD simulation has been performed on Vpu/DLGPC/water, Vpu^{27-57}/DLGPC/water and Vpu^{51-81}/DLGPC/water systems at 1 atm normal pressure, room temperature and 22.9 mN/M surface tension. This MD study has reproduced many experimental observations, such as Vpu's three helices, the orientations of these helices and helix-loop-helix-turn motif of VpuCyto domain in the membrane environment well. The agreement indicates the effectiveness of using $NP_N\gamma T$ MD simulations in membrane protein structural studies when the simulation is used in conjunction with experimental observables. Furthermore, the amphipathicity of two helices in the VpuCyto domain is verified at the atomic level and detailed information about the hydrophobic/hydrophilic sides was revealed. CytoHelix1 is about 0.5 nm closer to the membrane surface than CytoHelix2 in full length Vpu, although both helices adopt parallel orientations toward the membrane surface. Different membrane propensities of these two helices indicate that in addition to the amphipathicity, other factors, such as the composition and length of the helix, may also influence the affinity of the helix for the membrane surface. Experimental study of the influence of peptide length on the interaction between amphipathic α-helical peptides and phosphatidylcholine liposomes shows that synthetic peptides 10–12 residues in length interact most effectively with the liposomes, but a six-residue peptide has no effect on liposome structure. [36] For the

orientation of CytoHelix2 toward the membrane surface, the simulations provide strong evidence for the possibility of different orientations of this helix in different peptides, as revealed by experiment. This indicates that the orientational variability of a cytoplasmic helix toward the membrane surface in different polypeptides may reflect this helix's relatively weak affinity for the membrane. The closely associated relationship between the highly conserved loop region and membrane surface was first revealed here. Although the function of phosphorylation of Ser52 and Ser56 in degradation of CD4 cannot be inferred from this study, the phosphorylation may result in loose association between the loop and the membrane surface because the loop region cannot form a hydrogen bond with lipid head groups after phosphorylation. The Vpu tail region was found in close proximity to the membrane surface. The elucidation of the structure of VpuCyto domain might assist the study of the protein–protein interaction between Vpu and CD4 cytoplasmic domains, which is important in Vpu-induced CD4 degradation. In the Vpu/DLGPC/water Langmuir monolayer, the tilt angle of 34 lipids associated with Vpu is similar to that of lipids in the pure DLGPC/water system. However, the lipids located between the VpuTM helix and CytoHelix1 are pushed up by Vpu, and the P–N tilt angle for the head group of these lipids is increased at the same time. The VpuTM domain usually causes more disorder in its neighboring lipid acyl chains than the VpuCyto domain. This suggests that lipid acyl-chains and head groups may exhibit conformational flexibility when the protein–lipid interaction is strong. Under the conditions used, the lipids not associated with the Vpu maintain essentially the conformational characteristics of those in a pure DLGPC/water Langmuir monolayer. This MD simulation has not only reproduced Vpu structural characteristics obtained from experiment, but has also yielded detailed complementary knowledge on its secondary structure and topology in the membrane/water environment and Vpu–lipid interaction at the atomic level. In a future MD study, the Vpu structure obtained from this work may be helpful in assembling a Vpu channel to reveal the virion-release function of the VpuTM domain. For other membrane proteins with known structural characteristics probed by various experimental techniques, this MD approach may also be applicable to supply more detailed structure and interaction information.

Acknowledgements This work was partially supported by National Institute of General Medical Science Program Project Grant PO1 GM56538.

References

1. Maldarelli F, Chen M, Willey RL, Strebel K (1993) J Virol 67:5056–5061
2. Schubert U, Schneider T, Henklein P, Hoffmann K, Berthold E, Hauser H, Pauli G, Porstmann T (1992) Eur J Biochem 204:875–883
3. Schubert U, Henklein P, Boldyreff B, Wingender E, Strebel K, Porstmann T (1994) J Mol Biol 236:16–25
4. Yedavalli VRK, Husain M, Horodner A, Ahmad N (2001) AIDS Res Hum Retroviruses 17:1089–1098
5. McCormick-Davis C, Dalton SB, Singh DK, Stephens EB (2000) AIDS Res Hum Retroviruses 16:1089–1095
6. Henklein P, Kinder R, Schubert U, Bechinger B (2000) FEBS Lett 482:220–224
7. Marassi FM, Ma C, Gratkowski H, Straus SK, Strebel K, Oblatt-Montal M, Montal M, Opella SJ (1999) Proc Natl Acad Sci USA 96:14336–14341
8. Wray V, Kinder R, Fedearu T, Henklein P, Bechinger B, Schubert U (1999) Biochemistry 38:5272–5282
9. Paul M, Mazumder S, Raja N, Jabbar MA (1998) J Virol 72:1270–1279
10. Schubert U, Ferrer-Montiel AV, Oblatt-Montal M, Henklein P, Strebel K, Montal M (1996) FEBS Lett 398:12–18
11. Bour S, Perrin C, Akari H, Strebel K (2001) J Biol Chem 276:15920–15928
12. Bour S, Geleziunas R, Wainberg MA (1995) Microbiol Rev 59:63–93
13. Bour S, Schubert U, Strebel K (1995) J Virol 69:1510–1520
14. Schubert U, Bour S, Ferrer-Montiel AV, Montal M, Maldarelli F, Strebel K (1996) J Virol 70:809–819
15. Tiganos E, Friborg J, Allain B, Daniel NG, Yao X, Cohen ÉA (1998) Virology 251:96-107
16. Chen M, Maldarelli F, Karczewski MK, Willey RL, Strebel K (1993) J Virol 67:3877-3884
17. Margottin F, Benichou S, Durand H, Richard V, Liu LX, Gomas E, Benarous R (1996) Virology 223:381–386
18. Wray V, Federau T, Henklein P, Klabunde S, Kunert O, Schomberg D, Schubert U (1995) Int J Peptide Protein Res 45:35–43
19. Federau T, Schubert U, Floßdorf J, Henklein P, Schomburg D, Wary V (1996) Int J Peptide Protein Res 47:297–310
20. Willbold D, Hoffmann S, Rösch P (1997) Eur J Biochem 245:581–588
21. González ME, Carrasco L (1998) Biochemistry 37:13710–13719
22. Bechinger B (2000) Phys Chem Chem Phys 2:4569–4573
23. Ewart GD, Sutherland T, Gage PW, Cox GB (1996) J Virol 70:7108–7115
24. Sun F (2002) Biophys J 82:2511–2519
25. Sayle RA, Milner-White EJ (1995) Trends Biochem Sci 20:374–376
26. Brooks BR, Bruccoleri RE, Olafson BD, States DJ, Swaminathan S, Karplus M (1983) J Comput Chem 4:187–217
27. Mackerell AD, Bashford D, Bellott M, Dunbrack RL, Evanseck JD, Field MJ, Fischer S, Gao J, Ha S, Joseph-McCarthy D, Kuchnir L, Kuczera K, Lau FTK, Mattos C, Michnick S, Ngo T, Nguyen DT, Prodhom B, Reiher WE, Roux B, Schlenkrich M, Smith JC, Stote R, Straub J, Watanabe M, Wiórkiewicz-Kuczera J, Yin D, Karplus M (1998) J Phys Chem B 102:3586–3616
28. Nosé S (1984) J Chem Phys 81:511–519
29. Hoover WG (1985) Phys Rev A 31:1695–1697
30. Zhang Y, Feller SE, Brooks BR, Pastor RW (1995) J Chem Phys 103:10252–10266
31. Forrest LR, Tieleman DP, Sansom MSP (1999) Biophys J 76:1886–1896
32. Ma C, Marassi FM, Jones DH, Straus SK, Bour S, Strebel K, Schubert U, Oblatt-Montal M, Montal M, Opella SJ (2002) Protein Sci 11:546–557
33. Bechinger B (2001) FEBS Lett 504:161–165
34. Segrest JP, De Loof H, Dohlman JG, Brouillette CG, Anantharamaiah GM (1990) Proteins 8:103–117
35. Kaiser ET, Kézdy FJ (1987) Annu Rev Biophys Biophys Chem 16:561–581
36. McLean LR, Hagaman KA, Owen TJ, Krstenansky JL (1991) Biochemistry 30:31–37